

Designing and development of electroactive Copper (II) complex with 2-[[4-hydroxy-3-[(Z)-phenyldiazenyl]phenyl](4-hydroxyphenyl) methyl]benzoic acid for selective determination of Catechol

S R Priyanka and K P Latha*

Department of P.G. Studies and Research in Chemistry, Sahyadri Science College, Shivamogga-577 203, Karnataka (S), INDIA

*E mail: kplatha11@gmail.com, priyankasr12345@gmail.com

Received: 11 July 2021/ Accepted: 6 September 2021 / Published: 10 October 2021

The new class Copper (II) complex of 2-[[4-hydroxy-3-[(Z)-phenyldiazenyl]phenyl](4-hydroxyphenyl)methyl]benzoic acid (Cu-PABC) has been well designed and accomplished. Fourier transform infrared spectroscopy, Mass spectra and UV spectra confirmed the structure of the title compound. The synthesized Cu-PABC was used to enhance the electropolymer on the carbon paste electrode (Poly(Cu-PABC)/MCPE) by using Cyclic voltammetric (CV) technique. Poly(Cu-PABC)/MCPE was developed into a selective, sensitive and repetitive electrochemical technique for the electroanalysis of hydroquinone (HQ) and catechol (CC). The reconstituted electrode reduces overpotential and promotes HQ and CC oxidation. The influence of scan rate measurement and concentration investigations indicates that analyte diffusion for CC and adsorption for HQ controls the electrode process. CV and differential pulse voltammetric (DPV) approaches were used to selectively separate HQ and CC in a binary relationship. The CV and DPV methods separated the high oxidation peak potentials for HQ – CC by around 0.114 V and 0.118 V, respectively. The peak potential differences were large enough to determine HQ and CC discretely. The lowest CC detection limit was 6.53 μ M and 7.3 μ M for HQ. The voltammetric parting of dihydroxy benzene isomers in the two-fold organization by CV method achieved by Poly(Cu-PABC)/MCPE; this function delivers easily and simple process for modifying the carbon paste electrode(CPE).

Keywords: Poly(Cu-PABC)/MCPE, Hydroquinone, Catechol, differential pulse voltammetry, cyclic voltammetry

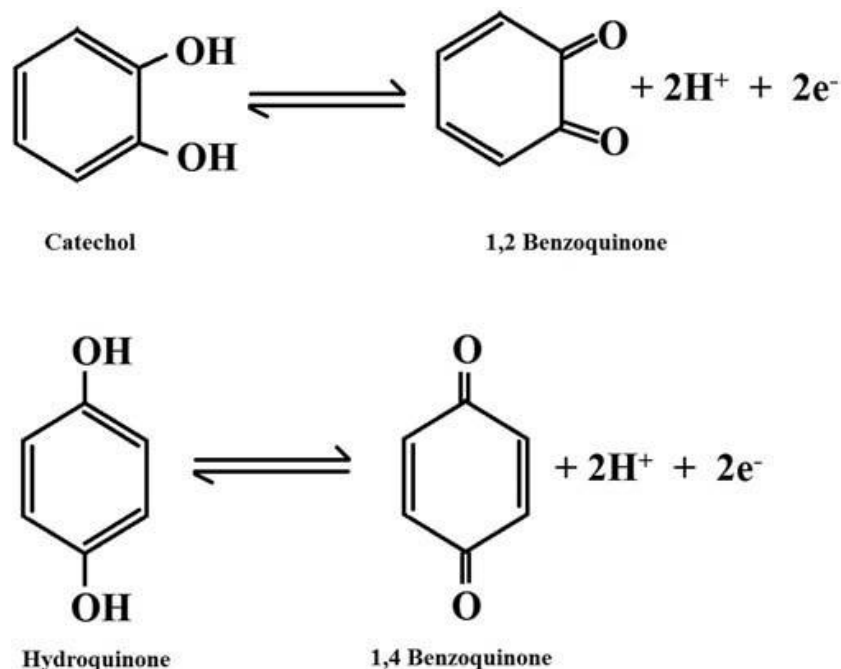
1. INTRODUCTION

The azo groups (N=N) complex organic structures with chromophore groups that increase solubility, improve substrate adhesion and most importantly electrochemically measurement with improved reaction time and sensory processing [1-7]. There are more than 3000 azo dyes used

worldwide, and they account for 65% of the commercial dye market and other uses in various field. Hydroquinone (HQ, 1,4-dihydroxybenzene) and catechol (CC, 1,2-dihydroxybenzene) are two important isomers of phenolic moiety broadly used in pharmaceutical industry, food, pigment, and photographic chemicals, antioxidants, properties oil refineries, coal tar, leather and paint [8-11]. Any of these can be introduced into the atmosphere during the repair and operation phases, which cause damage to the environment. Because of their high toxicity and low corrosion [12], the development of a fast, simple and reliable analytical technique for determining dihydroxybenzene isomers is important. At the same time limitations of these isomers, there were few research articles available. Spectrophotometry [13], using high-performance liquid chromatography (HPLC) [14], electrochemiluminescence [15], and pH-based-flow injection analysis [16] are examples.

Researchers have been drawn to electroanalytical methods in order to improve electrochemical sensors for the detecting electroactive compounds [17-21]. Voltammetric techniques have become very popular in recent decades due to their ease of use, high sensitivity, low cost, and rapid response [22-25]. Because of its applied recompenses such as large potential window, easy grinding, efficient modification and low cost, carbon paste electrode (CPE) is the preferred functional electroanalysis of active molecules over other solid electrodes [26, 27]. However, in CPE, the voltammetric response to electroactive chemicals is the least selective and sensitive. In addition, the obtained voltammogram is broad due to the slow transport of the electron and analysis of the target analyte when there is a interferences may be a difficult task at times [28]. Targeted molecular studies, many modification processes and methods have been recorded [29-32]. Various Nanoparticles [33, 34], ionic liquid [35], inorganic substances [36], electropolymerization [37-41] surfactants [42, 43] and carbon nanotubes [44] have also been used to modify CPE.

In BCPE, both HQ and CC receive anodic oxidation with almost the same potentials owing to their comparable structure and possessions [22]. Individual detection of these isomers is frequently challenging, resulting in a voltammetric response that is overlapped and has limited sensitivity and selectivity. The fouling effect of CPEs is caused by the deposition of oxidized compounds on the surface. As a result, modifying CPEs to address this issue is a promising and emerging field of electroanalytical science [22, 38-39]. There have been several CPEs records modified to attain the goal of selective and sensitive analysis of these isomers [45-48]. The current work we focus on the synthesize Copper (II) complex of 2-[[4-hydroxy-3-[(Z)-phenyldiazenyl]phenyl](4-hydroxyphenyl)methyl] benzoic acid (phenolphthalein azo based Copper (II) complex) (Cu-PABC) which has a conventional method and provides comprehensive modification of the CPE by electropolymerisation by Cu-PABC, which is used for voltammetric resolution of CC and HQ. Cu-PABC exhibited significantly a saddle like distorted structure with admirable yield. The ultimate structure of Cu-PABC was characterized by FTIR spectra, Mass Spectra and UV spectra. Cu-PABC electropolymerisation of carbon paste electrode (Poly(Cu-PABC)/MCPE) demonstrates the sensitivity, stability, selectivity and duplicability of the result for the voltammetric resolution of 2-dihydroxy benzene isomers. CC and HQ oxidation mechanism is displayed in Scheme 1. It indicates on Poly(Cu-PABC)/MCPE the CC undergoes oxidation to form 1,2 benzoquinone and backward 1,2 benzoquinone undergo reduction to form CC as well as HQ undergo oxidation to form 1,4 benzoquinone and this 1,4 benzoquinone undergo reduction in the backward direction to form HQ



Scheme 1. Oxidation mechanism of CC and HQ.

2. EXPERIMENTAL

2.1. Reagents

Himedia provided the Catechol (CC), hydroquinone (HQ), Aniline, sodium nitrite, ethanol, sodium carbonate, $\text{CuCl}_2 \cdot 2\text{H}_2\text{O}$ and 2-[bis(4-hydroxyphenyl)methyl]benzoic acid. In double distilled water, stock solutions of 25×10^{-4} M HQ and 25×10^{-4} M CC were prepared. Phosphate buffer solution (PBS) of the uniform ionic strength (0.2 M) was retained, while the chosen pH was produced by mixing the suitable ratio of $\text{NaH}_2\text{PO}_4 \cdot \text{H}_2\text{O}$ and Na_2HPO_4 . Merck supplied dimethyl formamide; the stock solution of Cu-PABC was prepared by dissolving in dimethyl formamide and fine graphite powder with a particle size of 50 μm , while Himedia provided silicone oil for CPE. All of the compounds are of analytical quality and are used in the manner provided, without any additional cleaning.

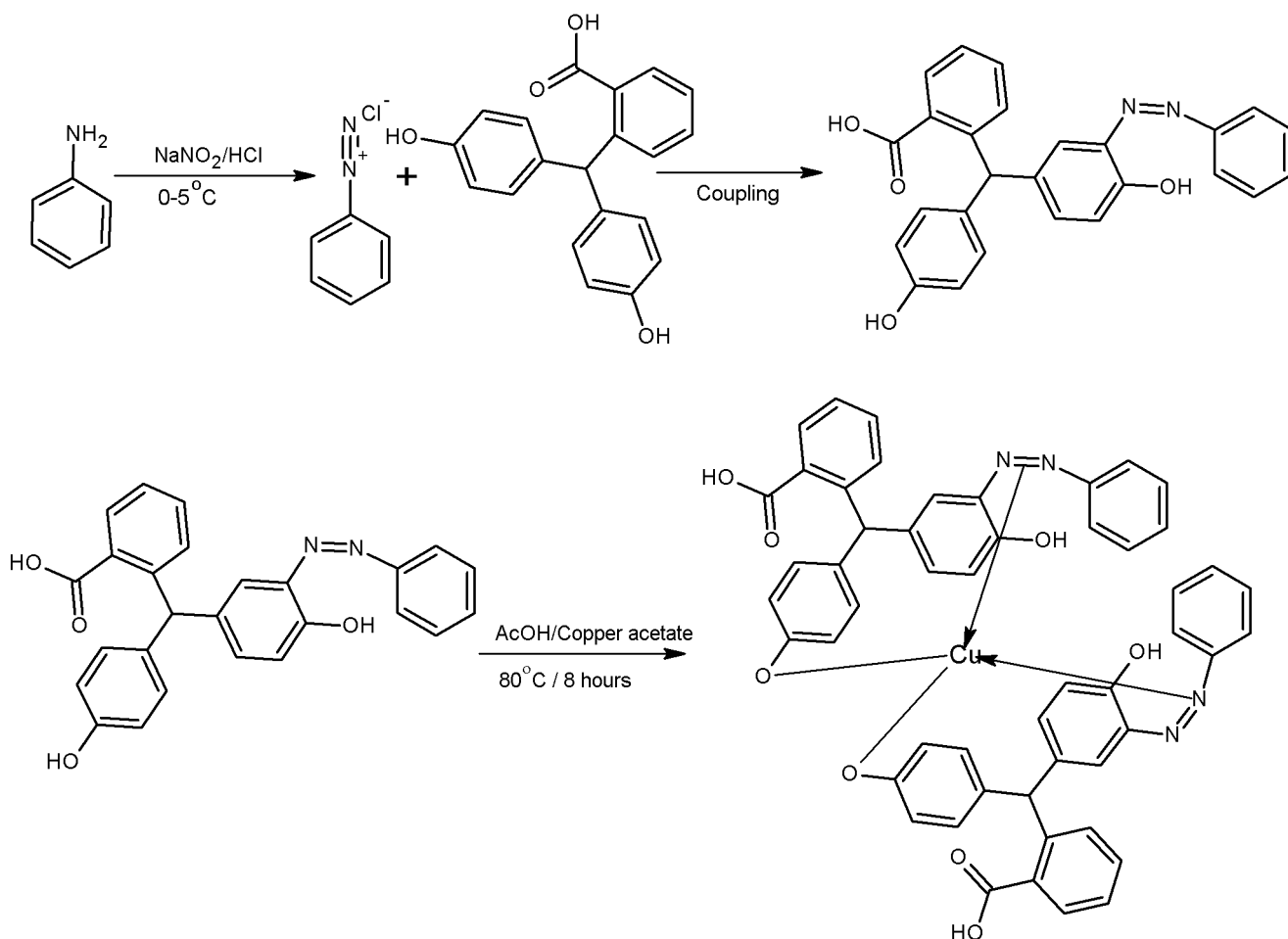
2.2. Equipment

Electrochemical studies were performed using the CHI-660c (CH Instrument-660 workstation) embedded in a standard three electrode cell. The saturated calomel electrode (SCE) is a reference electrode, the platinum wire is used as counter electrode, and bare carbon paste electrode (BCPE) or Poly(PBA)/MCPE or Poly(Cu-PABC)/MCPE is used as a working electrode. At a temperature of 25 ± 0.5 °C, potentials of all redox samples were measured vs the SCE.

2.3. Synthesis of Metal Complexes

Diazotization: Aniline cooled at 0-5 °C and an equimolar solution of aqueous sodium nitrite (NaNO_2 , 0.7g 0.01 mol) was added slowly with constant stirring. After adding completely, the stirring continued for 30 minutes. Excess NaNO_2 was destroyed by adding required amount of urea. The pH of the reaction mixture was maintained at 6 by adding a cold water solution of sodium carbonate. In this solution, 2-[bis(4-hydroxyphenyl)methyl]benzoic acid (1.88 g, 0.01 mol, taken in 10 ml dry alcohol) was added in portions while maintaining a temperature of 0-5 °C at pH-6 for 2 hours. The resulting dye was filtered, washed, dried, and then recrystallized from appropriate solvent. The purity of the compound was tested with thin layer chromatography (TLC).

(0.268 g, 2 mmole) of 2-[[4-hydroxy-3-[(Z)-phenyldiazenyl]phenyl](4-hydroxyphenyl)methyl]benzoic acid (PBA) ligand liquefied in ethanol was deliberately incorporated by stirring 0.085 g (1 mmole) of $\text{CuCl}_2 \cdot 2\text{H}_2\text{O}$ stored for 8 hours at 80 °C. The reaction of the mixture was cooled and black color of the precipitate was formed, filtered and washed in ounces number (1:1) of H_2O : ethyl alcohol solution as indicated in scheme.2.



Scheme 2. Synthesis of Cu-PABC.

2.4. Working electrode Preparation

BCPE was equipped rendering to the described process [22]. Electropolymerisation of Cu-PABC on the surface of BCPE was performed using CV method in aqueous solution holding 10 μM Cu-PABC in 0.2 M PBS of pH 5.8. Electropolymerization was obtained with the development of a flick that produced between -0.5 V to +1.8 V with a scan rate of 0.1 V s^{-1} for 15 cycles. Later electrode was carefully washed by double distilled water. Using the 10 μM PBA ligand, In the same condition Poly(PBA)/MCPE was developed.

3. RESULTS AND DISCUSSION

3.1. Characterization of Cu-PABC

FT-IR, UV-Vis, and mass spectra were used to characterize the newly synthesized PBA and Cu-PABC. The infrared spectral data of the PBA is shown in Figure.1 (fig.1) and Cu-PABC is shown in fig.2.

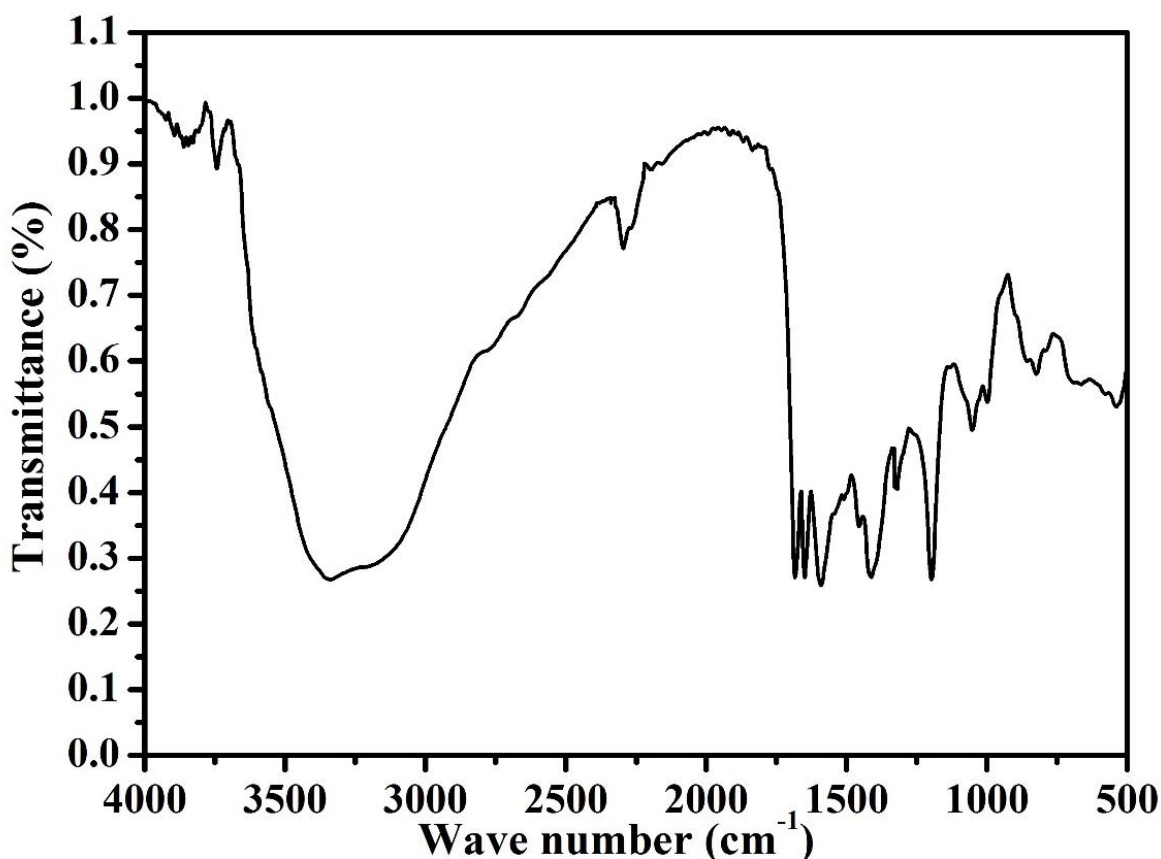


Figure 1. IR-spectra of PBA.

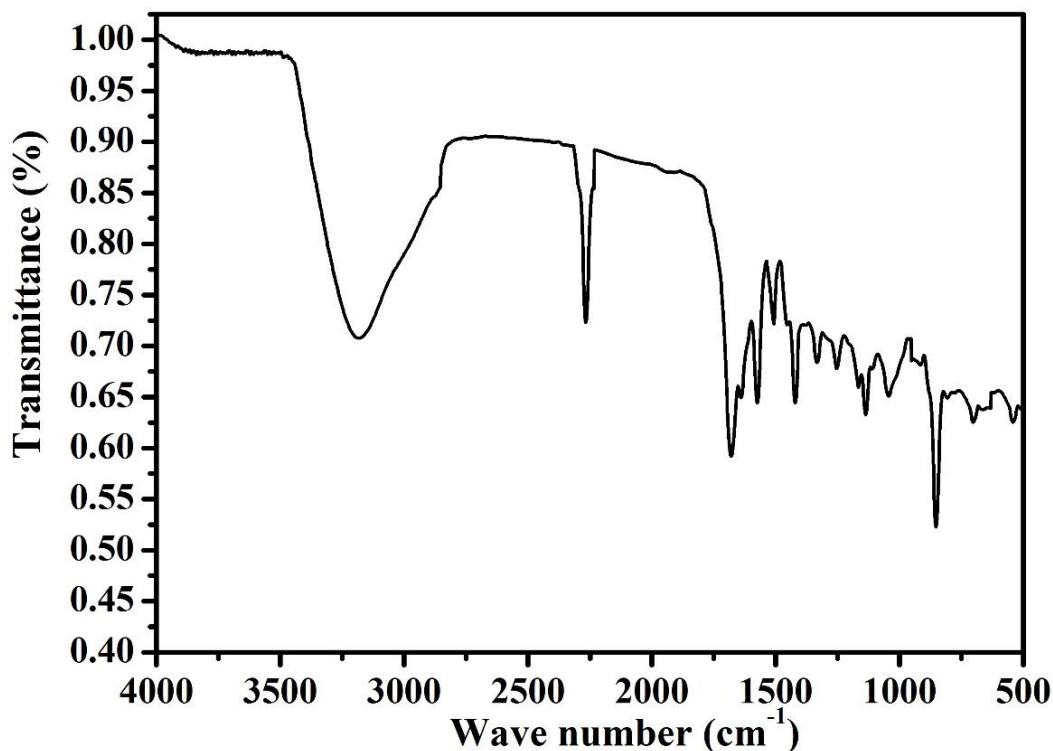


Figure 2. IR-spectra of Cu-PABC.

It can be seen that, by comparing the important indications of OH and COOH groups in the ligand PBA showing a broad band visible approximately 3350.89 to 3206 cm^{-1} and Cu-PABC showing a narrow broad band width of approximately 3200.17 to 3170.63 cm^{-1} assigned, decreasing wide band width of OH and COOH indicates that the complex formation with copper metal and ligand is shown in fig.1 and fig.2 respectively. For C=O group at 1688.37 cm^{-1} and 1682.31 cm^{-1} , A peak at 1412.68 cm^{-1} and 1424.79 cm^{-1} is assigned to N=N of azo group, aromatic CH peak appeared at 2296.58 cm^{-1} and 2265.52 cm^{-1} for ligand and complex are shown in fig.1 and fig.2 respectively. Cu-ligand peak appeared at 854.46 cm^{-1} as shown in fig.2. The IR spectrum of the complex and its compounds confirmed the proposed structure.

Mass spectrometry analysis (LCMS) of the PBA and Cu-PABC is shown in Fig.3 and fig.4 respectively. A molecular ion peak of ligand PBA with 424.44 calculated with Found 423.44. The molecular ion peak of Cu-PABC with calculated 910.42 and found 909.42 was in positive mode and confirmed the formation of complex.

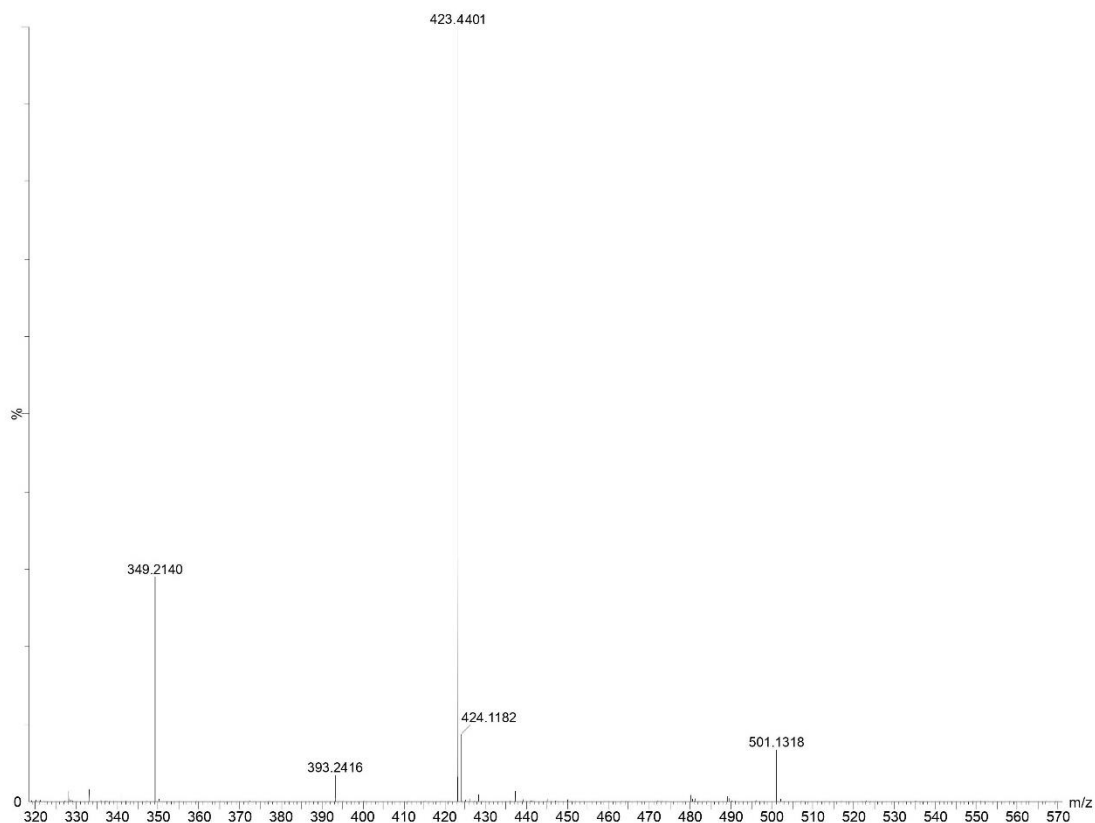


Figure 3. Mass-spectra of PBA.

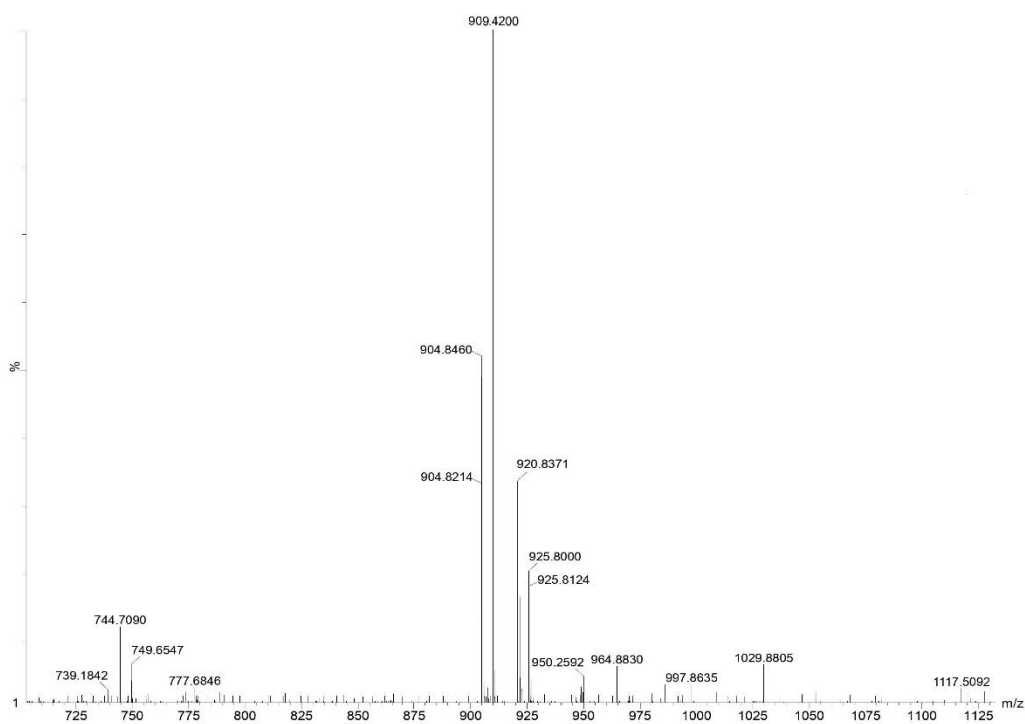


Figure 4. Mass-spectra of Cu-PABC.

3.2. Electronic Absorption Spectra

Electronic absorption shows are fruitful to establish the composition of the Cu-PABC and its ligand PBA shows the powerful demonstration of electronic absorption had to be in fig. 5. Electronic absorption spectrum governed by two intense bands namely UV region at 330.86 nm, 423.02 nm (Soret or B band), and Q band 478.05 nm for ligand and 333.56 nm, 409.97 nm (Soret or B band) & Q band 506 nm for complex respectively. The significant change in Q band splitting can detected is owing to the Q band absorptions of complexes are owed to $\pi \rightarrow \pi^*$ transitions from the maximum employed molecular orbital (HOMO) to the lowest unoccupied molecular orbital (LUMO) complex due to transition shows effective electronic transition between metal and ligand moiety and confirm the formation of the complex.

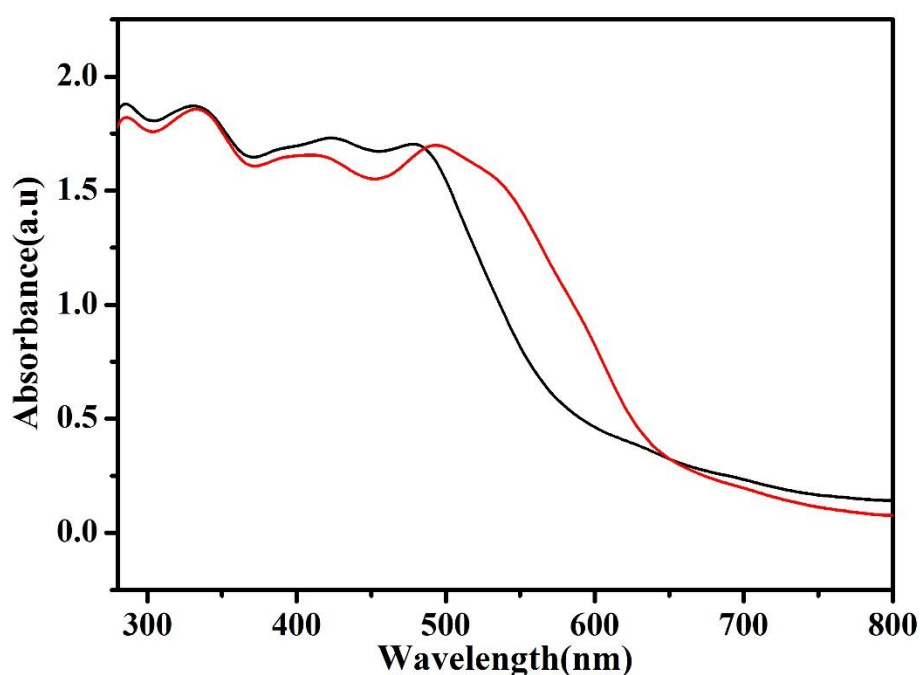


Figure 5. UV-Spectra of Cu-PABC and PBA ligand.

3.3. Electrochemical polymerization of Cu-PABC on BCPE

Poly(Cu-PABC)/MCPE was developed by scanning a 10 μM Cu-PABC solution in 0.2M PBS with a pH of 5.8 in an electrochemical cell at 15 cycles across a potential range of -0.5 V to +1.8 V at scan rate of 0.1 V s^{-1} . The currents of the anodic peak have risen at the beginning, as shown in Fig. 6A, showing the progress and development of an electroactive layer on the surface of BCPE. Later fourteen cycles, the peak current increase was generally stable and steady, indicating that polymerization growth had reached completion [49, 22]. Based on the experimental data obtained, the film thickness has a significant effect on the electrocatalytic potential in poly(Cu-PABC)/MCPE. Coverage is measured by varying the number of cycles performed on the BCPE (from 5 to 20 multiple cycles) and the electrocatalytic activity towards the oxidation of 50 μM CC in 0.2 M PBS with a pH of

7.4 was analyzed. Both the anodic and cathodic peak currents are increased over 15 multiple cycles, as shown in Fig. 6B. For this reason, fifteen cycles of electropolymerisation of Cu-PABC/MCPE were selected. Peak currents begin to decrease when the number of polymerizing cycles exceeds 15; increasing the thickness of the film inhibits the electron transfer method and decreases the oxidation phenomena. As a result, 15 cycles were selected as a sample for BCPE modification. In the present study, a possible range of -0.5 V to +1.8 V was considered. Because of the deficiency of the monomer free radical Cu-PABC, if the positive potential is less than 1.8 V, no polymer film is formed and a positive potential greater than 1.8 V promotes over-oxidation of the Cu-PABC monomer, resulting in degradation of the polymer film. If the initial potential was negative than the -0.5V will create distortion in the constant arrangement of the polymer film.

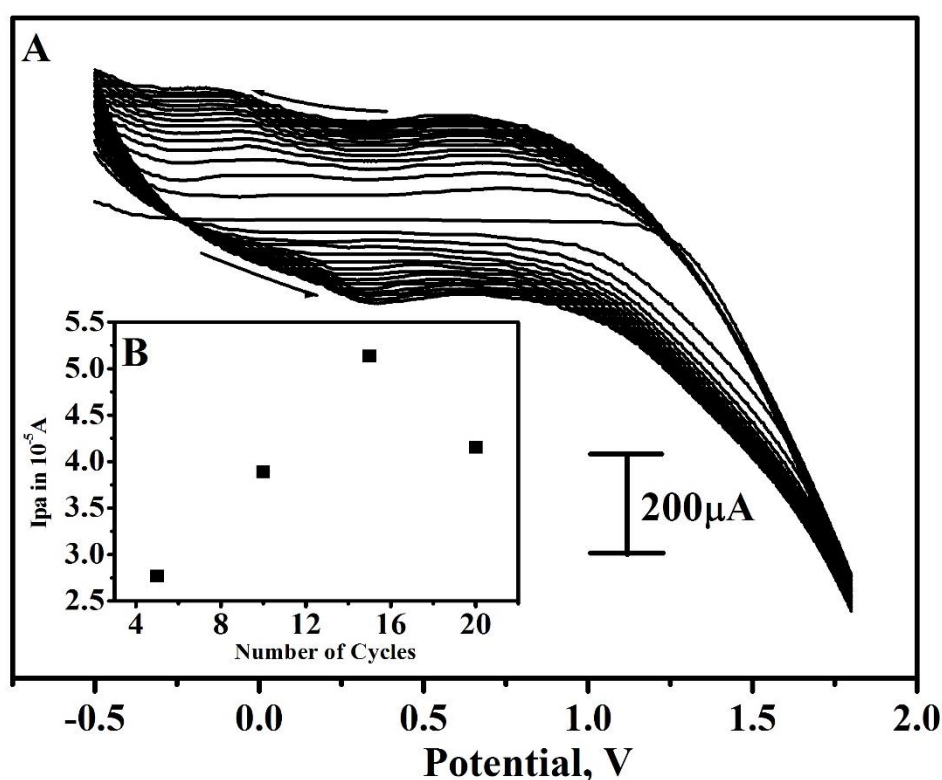


Figure 6. (A) Cyclic voltammograms for preparation of Poly(Cu-PABC)/MCPE. 10 μM Cu-PABC solution was taken in 0.2M PBS of pH 5.8 at 15 cycles with a scan rate of 0.1Vs^{-1} . (B) Graph of anodic peak current versus number of polymerization cycles (Ipa vs Number of cycles).

3.4. Electrochemical characterization of Poly(Cu-PABC)/MCPE and Poly(PBA)/MCPE using the typical potassium ferrocyanide system

The functional area of sensing electrode was examined by using the BCPE, Poly(PBA)/MCPE and Poly(Cu-PABC)/MCPE was studied using potassium ferrocyanide ($\text{K}_4[\text{Fe}(\text{CN})_6]$) as redox experiment in the process of CV technique as Fig.7. displays the cyclic voltammograms recorded with oxidation of 1mM $\text{K}_4[\text{Fe}(\text{CN})_6]$ in 1M potassium chloride (KCl) at Blank (no added

$K_4[Fe(CN)_6]$ (solid line), BCPE (dashed line), Poly(PBA)/MCPE(dash and dotted line) and Poly(Cu-PABC)/MCPE (dotted line) with a scan rate of 0.05 V s^{-1} . For BCPE low redox peak current was observed and 0.131 V be the redox peak potential difference, but for the Poly(PBA)/MCPE exhibited increase in redox peak current and 0.066 V would be the redox peak potential difference. Compare to BCPE and Poly(PBA)/MCPE, the Poly(Cu-PABC)/MCPE exhibited static increase in redox peak currents, with 0.046 V redox peak potential difference corresponding to the oxidation of $[Fe(CN)_6]^{4-}$ to $[Fe(CN)_6]^{3-}$. Poly(Cu-PABC)/MCPE showed reduction in over potential and improved sensitivity compare to BCPE and Poly(PBA)/MCPE. Poly(Cu-PABC)/MCPE was analyzed for different scan rates [0.05 to 0.5 Vs^{-1}]. The effective area of the electrodes in a reversible process can be determined using the Randles-Sevick equation (1) [35, 50]. These findings suggest that the surface morphology of the Poly(Cu-PABC)/MCPE is strongly affected, as well as the impact on the electrocatalytic activity of the Poly(Cu-PABC)/MCPE.

$$I_p = (2.69 \times 10^5) n^{3/2} A D^{1/2} C_0 \nu^{1/2} \text{ ----- (1)}$$

where, I_p is the peak current, A is the electroactive surface area (cm^2), n is number of electrons exchanged, C_0 is concentration of the electroactive species (mol cm^{-3}), D is coefficient of diffusion ($\text{cm}^2 \text{s}^{-1}$), ν is the scan rate (Vs^{-1}). The experimental relation of the oxidation peak currents with respect to the square root of the scan rate reveals the electrode process was diffusion controlled. From the slope I_{pa} versus $\nu^{1/2}$, the values of A were calculated to be 0.03642 cm^2 , 0.03252 cm^2 and 0.02829 cm^2 for Poly(Cu-PABC)/MCPE, Poly(PBA)/MCPE and BCPE respectively.

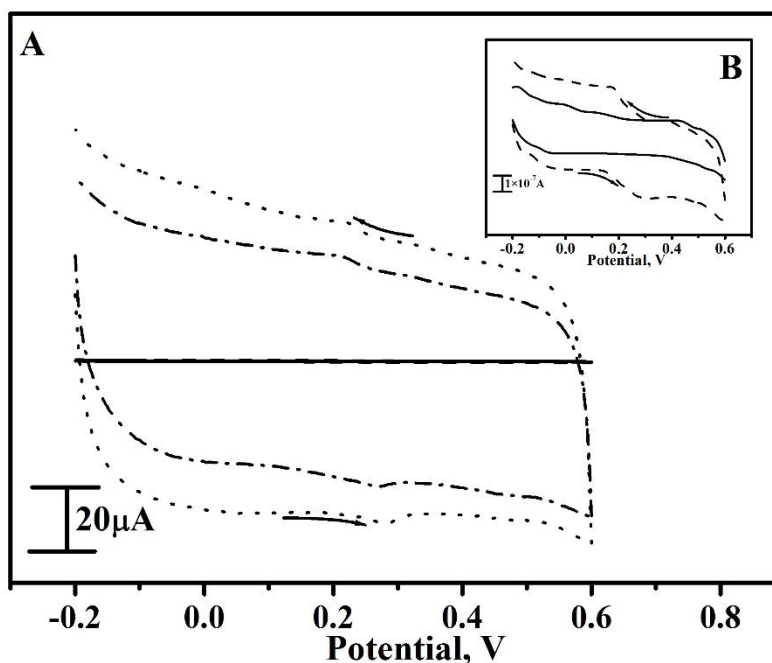


Figure 7. Cyclic voltammograms of $1 \text{ mM } K_4[Fe(CN)_6]$ in 1 M potassium chloride (KCl) at BCPE (solid line), BCPE (dashed line), Poly(PBA)/MCPE (dash and dotted line) and Poly(Cu-PABC)/MCPE (solid line) with a scan rate of 0.05 V s^{-1} .

3.5. Electrochemical study of CC at Poly(Cu-PABC)/MCPE

Cyclic voltammograms of $50\mu\text{M}$ CC for BCPE, Poly(PBA)/MCPE and Poly(Cu-PABC)/MCPE at 0.2 M PBS for pH 7.4 with a scan rate of 0.05 Vs^{-1} are shown in Fig. 8. CC demonstrates reduction and oxidation potentials in the low current signal with poor voltammetric response at BCPE (dash line), which was located at 0.188V and in Poly(PBA)/MCPE(dotted line) was located at 0.208V (Versus SCE). In the similar conditions, Poly(Cu-PABC)/MCPE (solid line) exhibit a remarkable increase in current signals and the oxidation potential is 0.169V. Compared to BCPE and Poly(PBA)/MCPE, redox peak currents increased about ten folds at Poly(Cu-PABC)/MCPE. As a result of these findings, it was found that the fabricated Poly(Cu-PABC)/MCPE had affinity for CC oxidation.

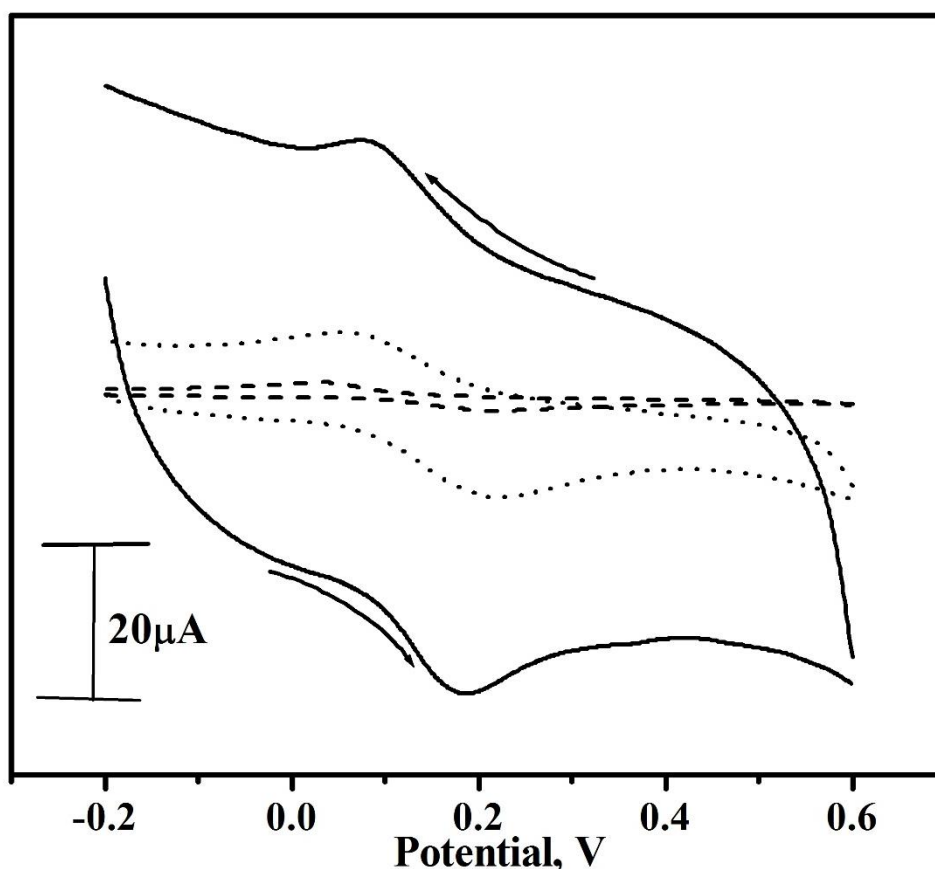


Figure 8. Cyclic voltammograms of $50\mu\text{M}$ CC in 0.2 M PBS of pH 7.4 at BCPE (dash line), Poly(PBA)/MCPE (dotted line) and The Poly(Cu-PABC)/MCPE (solid line) at scan rate of 0.05 V s^{-1} .

3.6. Effect of scan rate for CC

The $50\mu\text{M}$ CC at 0.2M PBS of pH 7.4 was resulted in Poly(Cu-PABC)/MCPE by CV technique for different scan rate as shown in the Fig. 9A. Poly(Cu-PABC)/MCPE obeys Randles-Sevcik equation and shows an scan rate increase with increment in redox peak currents through a

change in redox peak potentials. From the voltammograms plot the graph of anodic peak current versus square root of scan rate (I_{pa} vs $v^{1/2}$) shows straight line with a good linearity [51-53] as shown in Fig. 9B. The linear regression equation is I_{pa} (10^{-5} A) = $3.0639 \times 10^{-4}(C_0 10^{-5}$ M/L) + 6.0274×10^{-6} , ($r^2 = 0.9969$, N = 8). The graph of logarithm of anodic peak current versus logarithm of scan rate ($\log I_{pa}$ vs $\log v$) was designed and revealed in Fig. 9C. The analyzed value of slope is found to be 0.5061; it confirms that the process of electrode is controlled by diffusion of analytes [54-55].

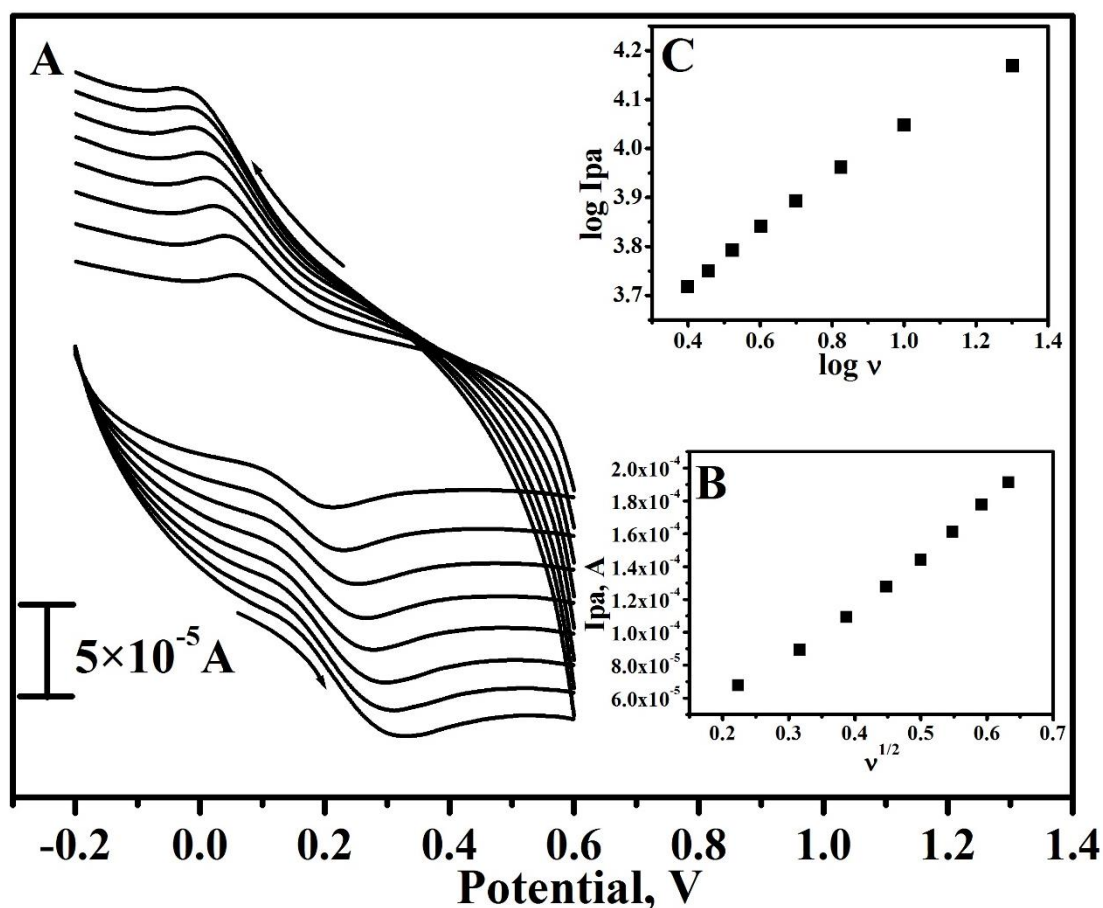


Figure 9. (A) Cyclic voltammograms of 50 μM CC in 0.2M PBS of pH 7.4 at Poly(Cu-PABC)/MCPE with different scan rate (0.05 V s^{-1} to 0.4 V s^{-1}). (B) Graph of I_{pa} vs $v^{1/2}$ (C) Graph of $\log I_{pa}$ vs $\log v$.

3.7. Effect of CC concentration

The electrocatalytic oxidation of CC is effected by its concentration change on Poly(Cu-PABC)/MCPE. Fig. 10A exhibits on increase in the concentration of CC from 5×10^{-5} M to 5×10^{-4} M the I_{pa} and I_{pc} goes on increases with a small shifting in the redox potentials. I_{pa} versus concentration of CC [CC] graph was designed as shown in Fig. 10B and exhibits a linearly straight line. The equation of linear regression is I_{pa} (10^{-5} A) = $0.2591(C_0 10^{-5}$ M/L) + 5.2133×10^{-5} , ($r^2 = 0.9988$, N = 10). Lowest limit of detection was determined [16, 22] and the limit of detection in the lower CC concentration was found to be $6.53 \mu\text{M}$ and the quantification limit was $21.76 \mu\text{M}$. The

Poly(Cu-PABC)/MCPE shown lower detection limit is compared with previous report in table 1 [22, 57–61].

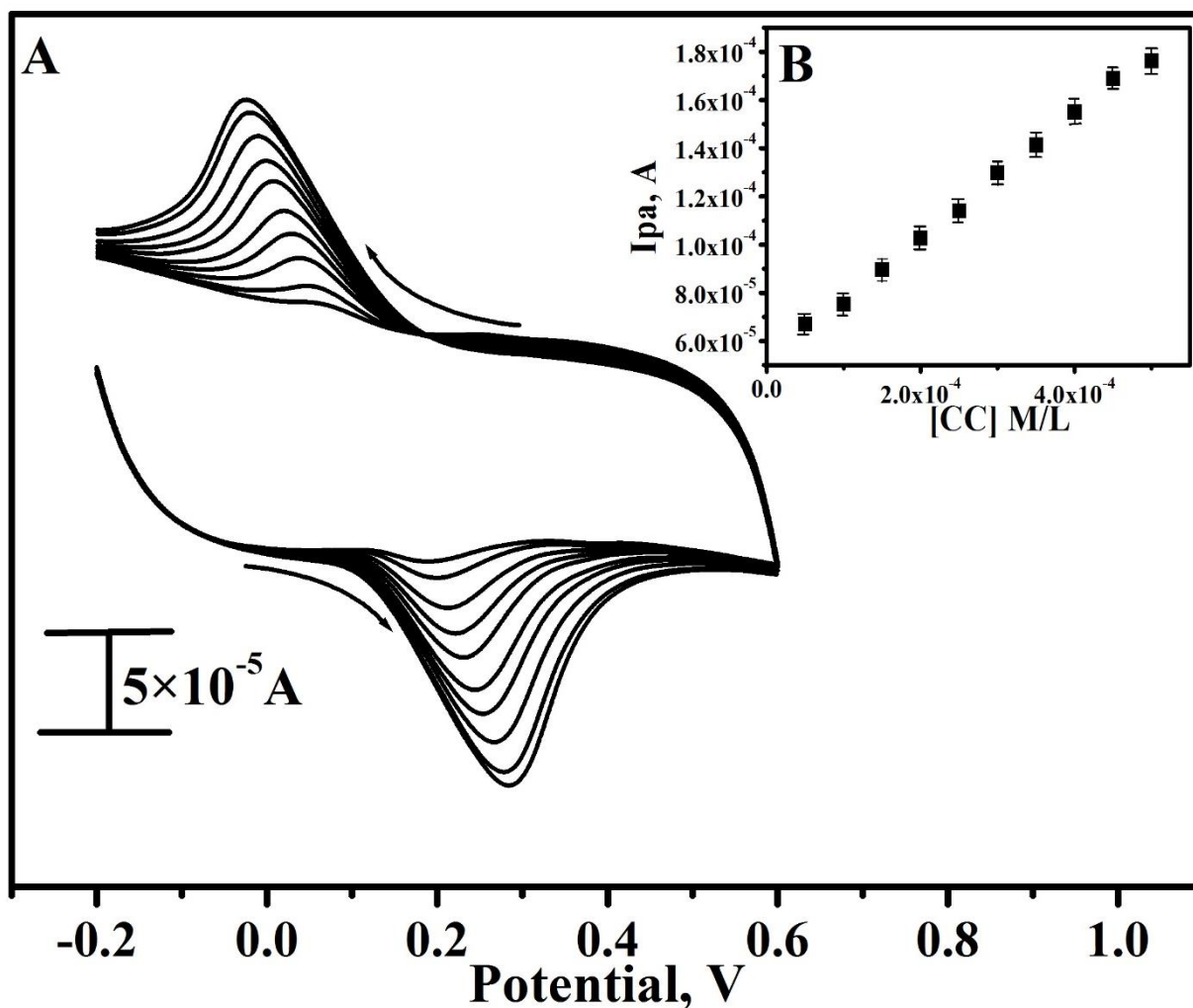


Figure 10. (A) Cyclic voltammograms of CC at 0.2M PBS of pH 7.4 at Poly(Cu-PABC)/MCPE at scan rate of 0.05 V s^{-1} with different concentrations ($5 \times 10^{-5} \text{ M}$ to $5 \times 10^{-4} \text{ M}$). (B) Graph of I_{pa} vs [CC] M/L

Table 1. Comparison of detection limits for other fabricated electrodes with Poly(Cu-PABC)/MCPE.

Working electrode	Limit of detection (μM)		Method	Reference
	CC	HQ		
Eosin Y/CPE	0.27	0.79	CV	[22]
(LDHf/GCE)	1.2	9.0	DPV	[57]
Poly(calmagite) MCPE	2.55	1.7	CV	[58]
PASA/MWNTs/GCE	1.0	1.0	DPV	[59]
PEDOT/GO modified electrode	1.6	1.6	DPV	[60]
Boron-doped graphene	0.2	0.3	DPV	[61]
Poly(Cu-PABC)/MCPE	6.53	7.3	CV	This Work

3.8. Effect of pH

The pH of the PBS plays an important role in the electrocatalytic oxidation of CC in Poly (Cu-PABC) / MCPE by peak current and peak potential. The consequence of the PBS pH value on CC determination in Poly(Cu-PABC)/MCPE was sensibly assessed at a pH range of 5.8–7.8. Fig. 11A exhibits cyclic voltammograms recorded with 50 μ M CC in Poly(Cu-PABC)/MCPE. The oxidation peak potential moves to a less positive potential from 0.290 V to 0.217 V depending on the pH. The anodic peak potential (E_{pa}) versus pH graph evidently shows that the E_{pa} is proportionally dependent on the pH value of 5.8–7.8 through a slope of 0.04 V/pH ($r^2 = 0.989$) as revealed in Fig. 11B also proposes when an same number of electrons and protons are interact in the redox mechanism [50].

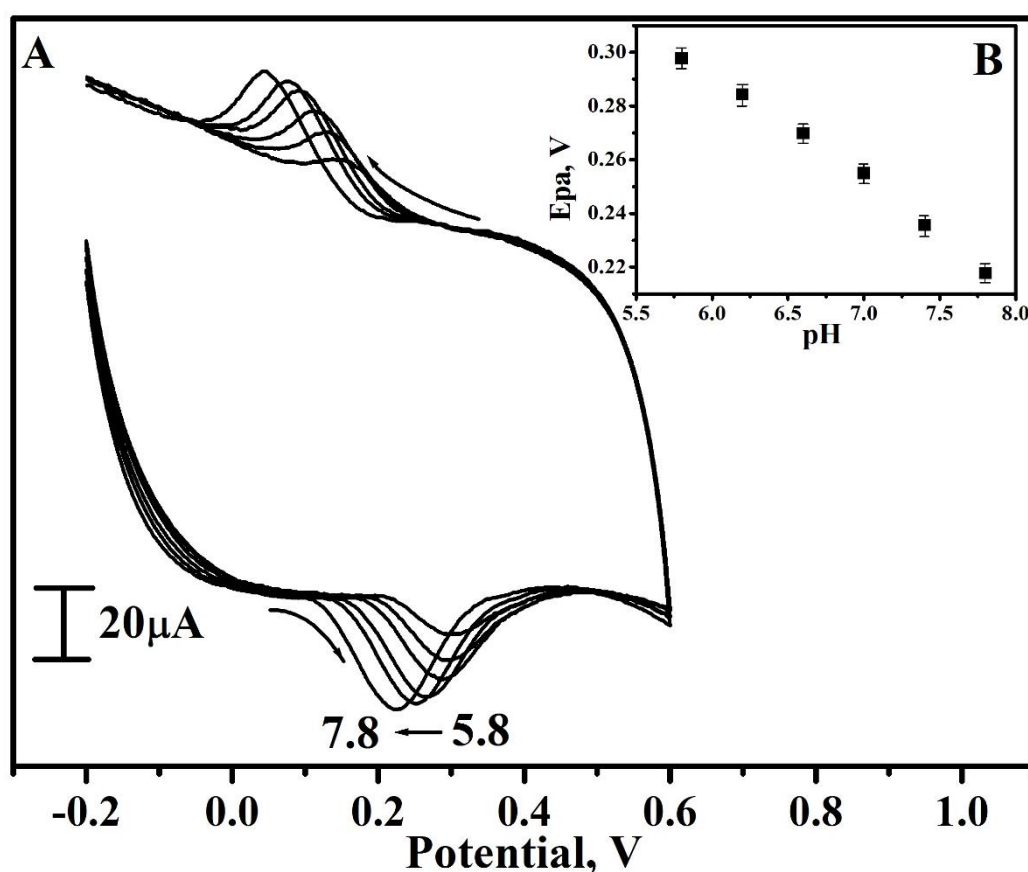


Figure 11. (A) 50 μ M CC Cyclic voltammograms in 0.2M PBS contain different pH (5.8 to 7.8) with scan rate of 0.05 V s⁻¹ at Poly(Cu-PABC)/MCPE. (B) Graph of E_{pa} versus pH.

3.9. Electrocatalytic oxidation of HQ at Poly(Cu-PABC)/MCPE

The oxidation of 50 μ M HQ at BCPE and Poly(Cu-PABC)/MCPE in 0.2M PBS of pH 7.4 with scan rate of 0.05 V s⁻¹ is shown fig. 12. It is evident from the figure that the oxidation potential of HQ at BCPE (dashed line) was wide range and low in sensitivity, the E_{pa} was available at approximately 0.095 V. Poly(Cu-PABC)/MCPE(solid line) and without adding any analyte is shown in dotted line

which confirms the redox peak only for the presence of analyte. It is also evident that the oxidation peak potential move to the negative side by reducing the over potential through improvement in peak current, Ep_a was present at 0.082 V. This shifting of oxidation peak potential and enhancement of the peak current signal approves the better electrocatalytic performance of Poly(Cu-PABC)/MCPE in relation to the oxidation of HQ.

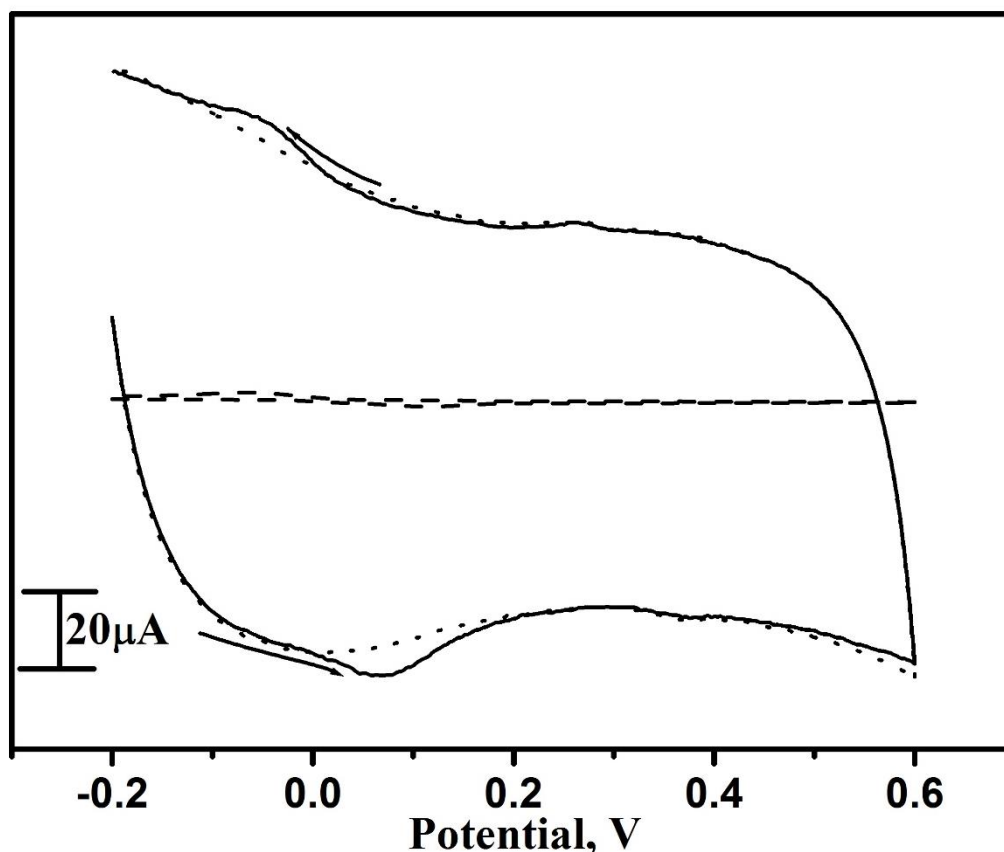


Figure 12. 50 μ M HQ Cyclic voltammograms in 0.2 M PBS of pH 7.4 at BCPE (dashed line) and Poly(Cu-PABC)/MCPE (solid line) with scan rate of 0.05 V s⁻¹.

3.10. Effect of scan rate on the peak current of HQ

Cyclic voltammograms were recorded with an oxidation of 50 μ M HQ in 0.2M PBS of pH 7.4 with different scan rate for Poly(Cu-PABC)/MCPE as shown in Fig. 13A. the increase in the scan rate leads to increase in redox peak currents with the shifting in the redox peak potentials at Poly(Cu-PABC)/MCPE. From the voltammogram the graph of the scan rate versus anodic peak current shows a linearly straight line as shown in fig.13B. The linear regression equation is $I_{pa} (10^{-5} A) = 0.0017(C_0 10^{-5} M/L) + 2.3165 \times 10^{-5}$, ($r^2 = 0.9959$, $N = 7$). A graph of the log I_{pa} vs log ν was plotted as shown in Fig. 13C. The calculated slope value is recorded (1.0728), which approves that the electrode process is controlled by adsorption of analyte [54, 62].

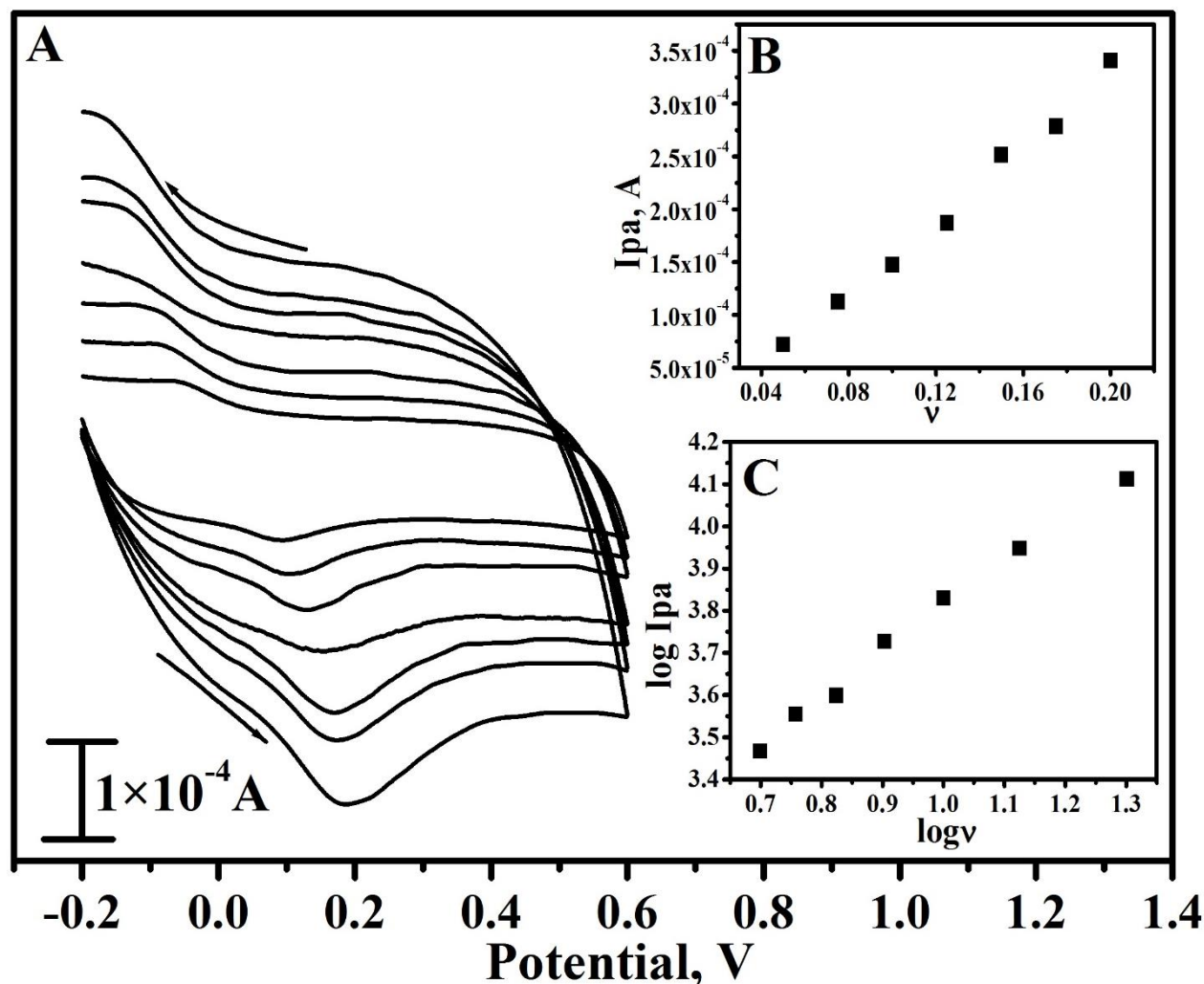


Figure 13. (A) Cyclic voltammograms of 50 μM HQ in 0.2M PBS of pH 7.4 at Poly(Cu-PABC)/MCPE with different scan rate (0.05 V s⁻¹ to 0.2 V s⁻¹). (B) Graph of I_{pa} vs v (C) Graph of log I_{pa} vs log v.

3.11. Effect of HQ concentration

Cyclic voltammograms were recorded at Poly(Cu-PABC)/MCPE in 0.2M PBS of pH 7.4. The concentration of HQ was analyzed in the range from 50 μM to 400 μM. As a result, increase the concentration has shown an improvement in HQ I_{pa} as revealed in fig. 14A. The graph of I_{pa} versus concentration of HQ (I_{pa} vs [HQ] M/L) has plotted as shown in Fig. 14B. It shows a linearly straight line with the linear regression equation $I_{pa} (10^{-5} \text{ A}) = 0.2318(C_0 10^{-4} \text{ M/L}) + 5.7201 \times 10^{-5}$, ($r^2 = 0.9957$ N = 8). The limit of quantification was 24.3 μM and LOD for HQ in the low concentration range was 7.3 μM the for Poly(Cu-PABC)/MCPE. The result obtained for Lower detection limit and it is compared with the previously found literatures shown in the table 1 [22, 57–61].

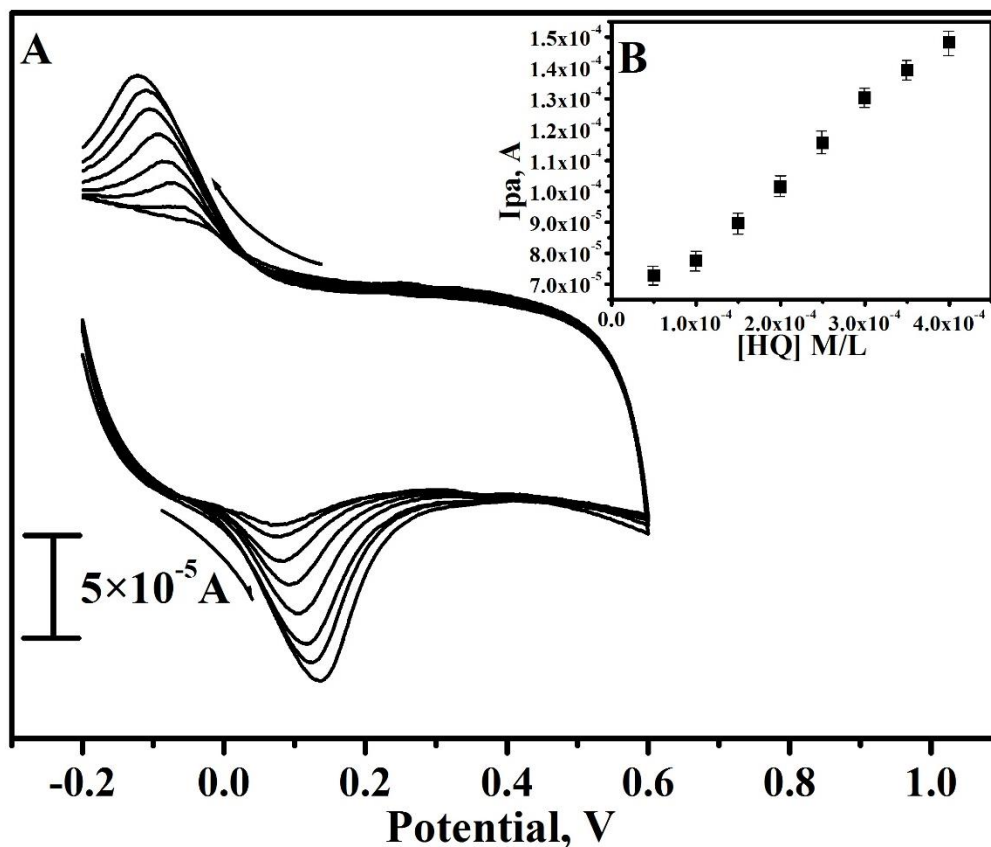


Figure 14. (A) Cyclic voltammograms of HQ in 0.2M PBS solution of pH 7.4 at Poly(Cu-PABC)/MCPE at scan rate of 0.05 V s^{-1} with different concentration ($0.5 \times 10^{-4} \text{ M}$ to $4 \times 10^{-4} \text{ M}$). (B) Graph of I_{pa} vs [HQ] M/L.

3.12. Voltammetric resolution of CC and HQ

The oxidation potential of phenolic isomers such as CC and HQ has almost the similar oxidation potential. The selective analysis of these isomers offers an overlapped voltammetric response with low selectivity and sensitivity at unmodified working electrodes. These isomers shows that selective identification is a very difficult task. Fig. 15 reveals that cyclic voltammograms recorded in a binary mixture of similar concentration of HQ and CC ($50 \mu\text{M}$) in 0.2 M PBS of pH 7.4 at BCPE (dashed line) and Poly(Cu-PABC)/MCPE (solid line) and without adding any analyte (dotted line) at Poly(Cu-PABC)/MCPE ensures that only an analyte shows redox peaks. The voltammetric response for BCPE is least selective and less sensitive, the overlapped oxidation was found to be at 0.177 V. In the similar condition Poly(Cu-PABC)/MCPE resolved cyclic voltammetric peaks for CC and HQ found to be 0.193 V and 0.073 V correspondingly. The peak to peak separation was 0.120V. This obtained result proved to be the best method for the determination of CC and HQ selectively.

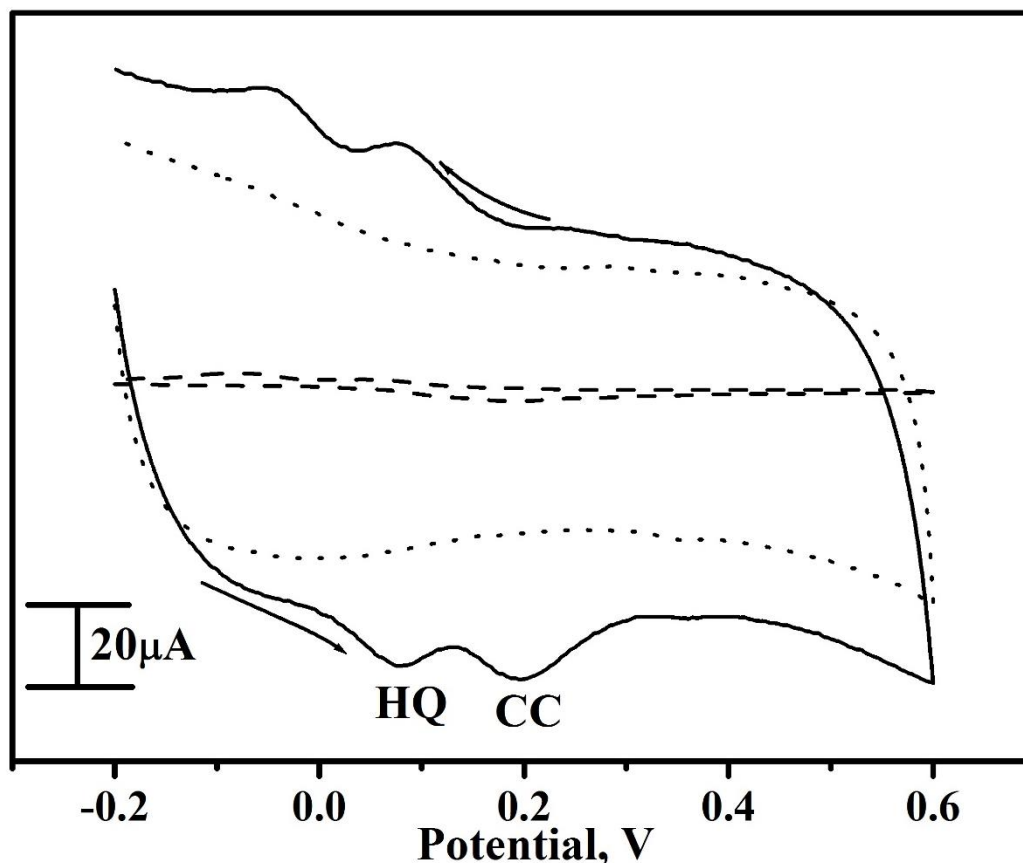


Figure 15. Cyclic voltammograms for simultaneous determination of 50 μM CC, 50 μM HQ at BCPE (dashed line) and Poly(Cu-PABC)/MCPE (solid line) at scan rate of 0.05 V s^{-1} .

Interference analysis were performed on combination of samples containing both CC and HQ at Poly(Cu-PABC)/MCPE. Concentration of one analyte is changing by kept the concentration of another analyte constant. From Fig. 16A it is observed that the peak current of CC was increased with increase in concentration from 0.5×10^{-4} M to 3.5×10^{-4} M by kept the concentration of HQ (50 μM) constant and the graph of I_{pa} vs [CC] M/L plotted as revealed in fig.16B and calculated the LOD obtained by 6.53 μM . Likewise, by changing the concentration of HQ from 0.5×10^{-4} M to 3.5×10^{-4} M, the peak current of HQ was increased at a constant concentration of CC (50 μM) as revealed in the fig. 17A and the graph of I_{pa} vs [HQ] M/L plotted as shown in the fig. 17B and calculated the LOD obtained by 7.3 μM . Due to the high sensitivity of the current and absence of the background current, Differential pulse voltammetry (DPV) was used for selective analysis of CC and HQ at 0.2 M PBS of pH 7.4 at both BCPE and Poly(Cu-PABC)/MCPE (Fig. 18). In the separated range of wide nature voltammogram observed at BCPE (solid line) and sensitivity was considerably lower at 0.102 V for CC and -0.02 for HQ, the peak separation was 0.122 V. For Poly(Cu-PABC)/MCPE (dotted line) without adding any analyte there is no oxidation peak appears but for same Poly(Cu-PABC)/MCPE (dashed line) confirms that the selected oxidation was detected at 0.106 V for CC and -0.016 V for HQ, the peak separation was 0.122 V. These results were found to be appropriate for the electroanalysis of CC and HQ in the mixture by DPV technique. From these results one can conclude that isomers oxidation is independent.

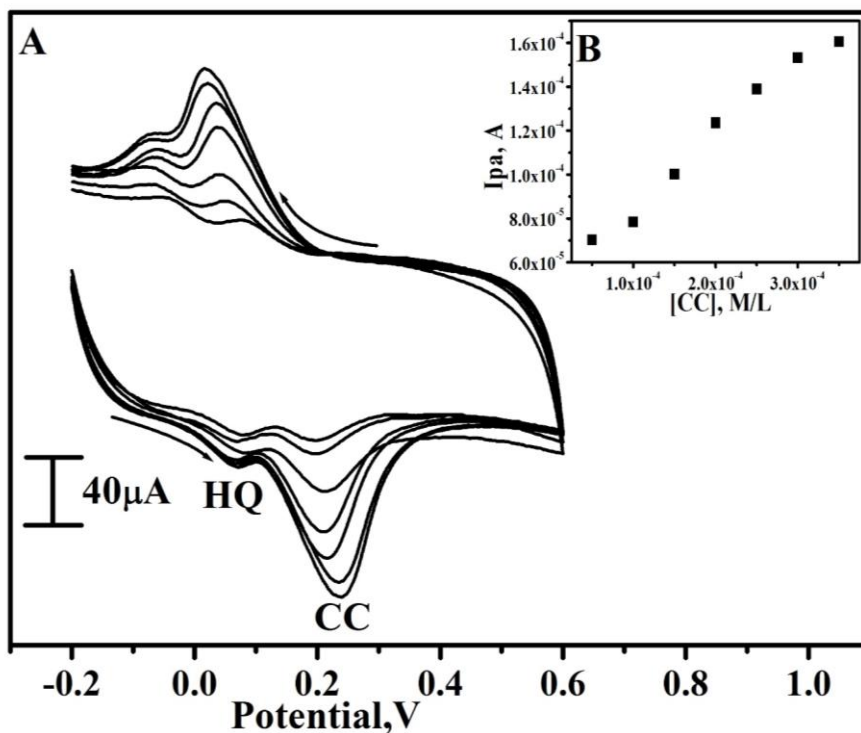


Figure 16. (A) Cyclic voltammograms of 0.5×10^{-4} M to 3.5×10^{-4} M CC in 0.2 M PBS of pH 7.4 in Presence of $50 \mu\text{M}$ HQ at Poly(Cu-PABC)/MCPE. (B) Graph of I_{pa} vs [CC] M/L.

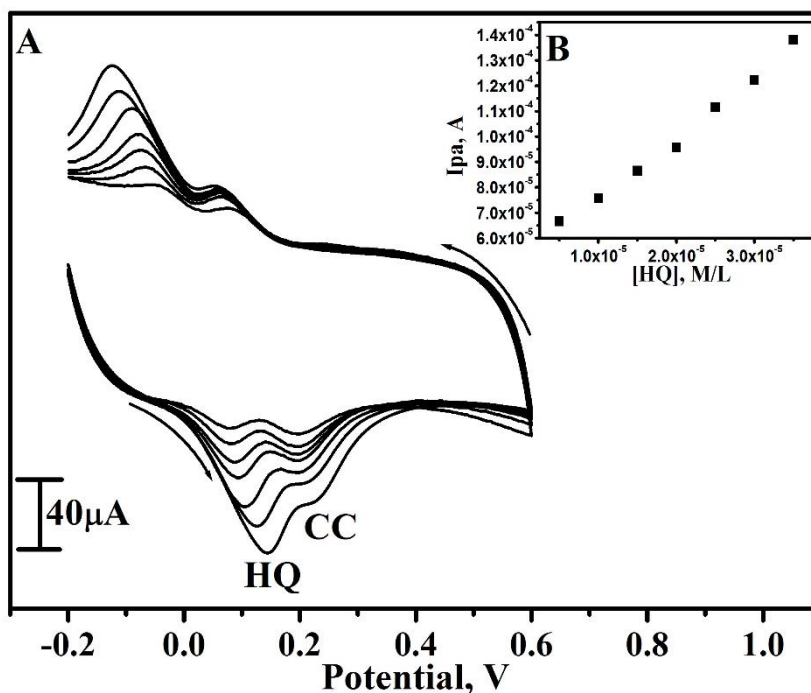


Figure 17. (A). Cyclic voltammograms of 0.5×10^{-4} M to 3.5×10^{-4} M HQ in 0.2 M PBS of pH 7.4 in Presence of $50 \mu\text{M}$ CC at Poly(Cu-PABC)/MCPE. (B) Graph of I_{pa} vs [HQ] M/L.

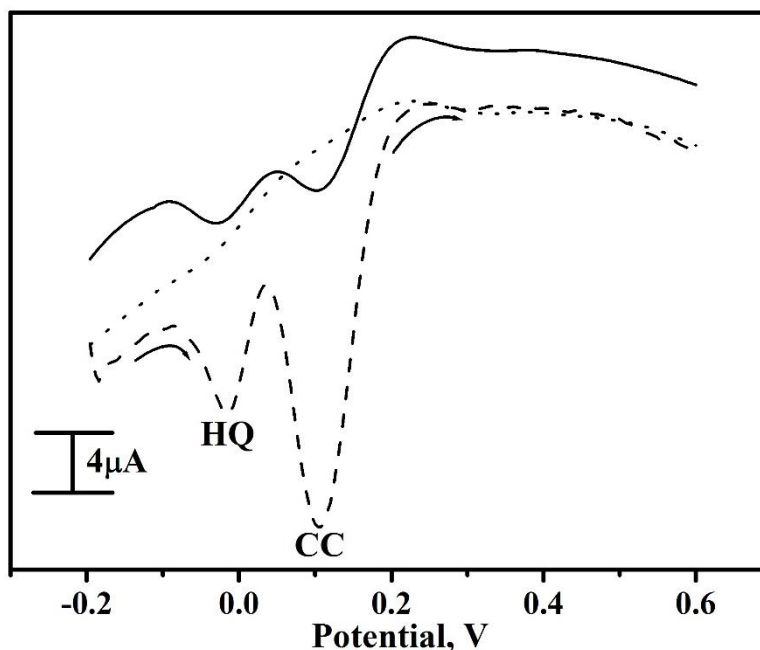


Figure 18. Differential pulse voltammogram obtained for 50 μ M CC, 50 μ M HQ in 0.2M PBS of pH 7.4 at BCPE (solid line) and Poly(Cu-PABC)/MCPE (dashed line).

3.13. Real sample analysis

In order to estimate the practicality of the prepared Poly(Cu-PABC)/MCPE in the real sample, the procedure described for [63] was employed for the determination of CC and HQ in lake water. Known concentrations of standard di-hydroxybenzene isomer solutions were prepared by diluting them with lake water and determined in the presence of PBS (pH 7.4) by the standard addition method. The obtained results are displayed as percentage recovery 99.1% – 105.9% and 98.4% – 103.3% in lake water were obtained for HQ and CC, respectively. This shows that the lake water used as the real sample does not affect the generation of oxidation peaks for dihydroxybenzene isomers.

4. CONCLUSIONS

Copper (II) complex of 2-[[4-hydroxy-3-[(Z)-phenyldiazenyl]phenyl](4-hydroxyphenyl)methyl] benzoic acid is synthesized by conventional method and characterised using various techniques. Synthesized product was used to modify the BCPE was reported by electropolymerised film Poly(Cu-PABC)/MCPE. This Poly(Cu-PABC)/MCPE shows good electrocatalytic performance in relation to the oxidation of HQ and CC by both CV and DPV techniques. The Poly(Cu-PABC)/MCPE shows that LOD is 6.53 μ M for CC and 7.3 μ M for HQ by CV method. So obtained results were in good agreement with the previous literature. Extended work was achieved by voltammetric determination of dihydroxy benzene isomers in the binary combination. Overall

Poly(Cu-PABC)/MCPE shows good sensitivity, selectivity, stability, reproducibility and antifouling property for dihydroxy benzene isomers. The real sample analysis for both CC and HQ shows the accepted recovery at Poly(Cu-PABC)/MCPE.

ACKNOWLEDGMENT

The author, S. R. Priyanka hereby acknowledges that she has the financial assistance for her Ph. D research from "National Fellowship & Scholarship for higher education of ST students" for the year 2017-18 and Ref. No: 201718-NFST-KAR-02320.

References

1. A.D. Towns, *Dyes Pigm.*, 42(1999)3.
2. E. Wagner-Wysiecka, N. Lukasik, J.F. Biernat and E. Luboch, *J. Inclusion Phenom. Macrocyclic Chem.*, 90(2018)189.
3. F.M. Shimizu, J.A. Giacometti, E.Luboch, J.F. Biernat and M. Ferreira, *Synth. Met.*, 159 (2009) 2378.
4. E. Leonard, F. Mangin, C. Villette, M. Billamboz and C. Len, *Catal. Sci. Technol.*, 6 (2016)379.
5. L. Androvic, J. Bartacek and M. Sedlak, *Res. Chem. Intermed.*, 42(2016) 5133.
6. D. Combita, P. Concepcion and A. Corma, *J. Catal.*, 311 (2014) 339.
7. C. G. Qin, Y. Li, H.L. Li, D.W. Li, W.W. Niu, X.Y. Shang and C.L. Xu, *Chin. J. Org. Chem.*, 33(2013) 444.
8. J. Wang, J. N. Park, X.Y. Wei and C.W. Lee, *Chem. Commun.*, 9 (2003) 628.
9. Y.H. Huang, J.H. Chen, X. Sun, Z.B. Su, H.T. Xing, S.R. Hu, W. Weng, H.X. Guo, W.B.Wu and Y.S. He, *Sens. Actuators, B*, 212 (2015) 165.
10. Y. Zhang, S. Xiao, J. Xie, Z. Yang, P. Pang and Y. Gao, *Sens. Actuators, B*, 204 (2014) 102.
11. W. Sun, Y. Wang, Y. Lu, A. Hu, F. Shi and Z. Sun, *Sens. Actuators, B*, 188 (2013) 564.
12. H. Yin, Q. Zhang, Y. Zhou, Q. Ma, T. Liu, L. Zhu and S. Ai, *Electrochim. Acta*, 56 (2011) 2748.
13. P. Nagaraja, R.A. Vasantha and K.R. Sunitha, *J. Pharm. Biomed. Anal.*, 25 (2001) 417.
14. P. Tuomainen and P.T. Mennistoe, *Eur. J. Clin. Chem. Clin. Biochem.*, 35 (1997) 229.
15. Y.G. Sun, H. Cui, Y.H. Li and X.Q. Lin, *Talanta*, 53 (2000) 661.
16. J.A.G. Mesa and R. Mateos, *J. Agric. Food Chem.*, 55 (2007) 3863.
17. M. Velmurugan, N. Karikalan, S.M. Chen, Y.H. Cheng and C. Karuppiah, *J. Colloid Interface Sci.*, 500(2017)54.
18. V.K. Gupta, A.K. Singh, S. Mehta and B. Gupta, *Anal. Chim. Acta*, 566 (2006) 5.
19. V.K. Gupta, A.K. Jain, P. Kumar, S. Agarwal and G. Maheshwari, *Sens. Actuators, B*, 113 (2006)182.
20. A.K. Jain, V.K. Gupta, L.P. Singh and J.R. Raison, *Electrochim. Acta*, 51 (2006) 2547.
21. V.K. Gupta, A.K. Singh, M.A. Khayat and B. Gupta, *Anal. Chim. Acta*, 590 (2007) 81.
22. P.S. Ganesh and B.E. K. Swamy, *J.Mol. Liq.*, 220 (2016) 208.
23. K.R. Mahanthesha and B.E. K. Swamy, *J. Electroanal. Chem.*, 703 (2013) 1.
24. L. Falat and H. Y. Cheng, *Anal. Chem.*, 54 (1982) 2108.
25. A. Rouhollahi, R. Rajabzadeh and J. Ghasemi, *Microchim. Acta*, 157(2007)139.
26. K. R. Mahanthesha, B. E. K. Swamy, U. Chandra, S. Reddy and K.V. Pai, *Chemical Sensors*, 4 (2014) 1.
27. K.R. Mahanthesha, B.E. K. Swamy, U. Chandra, S. S. Shankar and K.V. Pai. *J.Mol. Liq.*, 172 (2012) 119.
28. C.Y. Ge, M.M. Rahman, X.B. Li and J. J. Lee, *J. Electrochem. Soc.*, 163(2016) B556.
29. C. Rajkumar, B. Thirumalraj, S.M. Chen, P.Veerakumar and K.C. Lin, *Microchim. Acta*, 185(2018)395.

30. W. Huang, T. Zhang, X. Hu, Y. Wang and J. Wang, *Microchim. Acta*, 185(2018)37.
31. X.T. Yao, L.Q. Wen, S.Y. Rong and L.Q. Ying, *J.Chromatogr. A*, 1109 (2006)317.
32. X.M. Ma, Z.N. Liu, C.C. Qiu, T. Chen and H.Y. Ma, *Microchim. Acta*, 180 (2013) 461.
33. S. Reddy, B.E.K. Swamy and H. Jayadevappa, *Electrochim. Acta*, 61 (2012) 78.
34. K.Chetankumar, B.E. K. Swamy and H.S. Bhojya Naik, *Mater. Chem. Phys.*, 267(2021) 124610.
35. B. N. Chandrashekar, B. E. K. Swamy, N.B. Ashoka and M. Pandurangachar, *J.Mol. Liq.*, 165(2012)168.
36. Rekha, B.E.K. Swamy and P.S. Ganesh, *Anal. Bioanal. Electrochem.*, 7 (2015) 647.
37. J. Peng, Y. Feng, X.X. Han and Z.N. Gao *Microchim. Acta*, 183(2016)2289.
38. K. Chetankumar, B. E. K. Swamy and S.C. Sharma, *J. Electroanal. Chem.*, 849(2019)113365.
39. K. Chetankumar, B. E. K. Swamy and S.C. Sharma, *Microchem.J.*, 156(2020)104979.
40. J. K. Shashikumara, B. E. K. Swamy and K. Chetankumar, *Chem. Data Coll.*, 32(2021)100661.
41. U. Chandra, B. E. K. Swamy, K. R. Mahanthesha, C. C. Vishwanath and B. S. Sherigara, *Chemical Sensors*, 3 (2013)1.
42. U. Chandra, B.E. K. Swamy, K. R. Mahanthesha and J. G. Manjunatha, *Int. J. Curr. Adv. Res.*, 4(2015) 237.
43. S. Sharath Shankar, B. E. K. Swamy, K. R. Mahanthesha, C. C. Vishwanatha and M. Kumar, *Anal. Bioanal. Electrochem.*, 5 (2013)555.
44. J. Tashkhourian, B. Hemmateenejad, H. Beigzadeh, M. H. Sarvari and Z. Razmi, *J. Electroanal. Chem.*, 714 (2014) 103.
45. Y. Zhou, W. Tang, F. Dang, S. Chai and L. Zhang, *Colloids Surf. B*, 118 (2014) 148.
46. P.S. Silva, B.C. Gasparini, H.A. Magosso and A. Spinelli, *J. Braz. Chem. Soc.*, 24 (2013) 695.
47. S. Dong, P. Zhang, Z. Yang and T. Huang, *J. Solid State Electrochem.*, 16 (2012) 3861.
48. Q. Guo, J. Huang, P. Chen, Y. Liu, H. Hou and T. You, *Sens. Actuators, B*, 163 (2012) 179.
49. C. M. Kuskur, B.E. K. Swamy and H. Jayadevappa, *Ionics*, 24 (2018) 3631.
50. S. R. Priyanka and K. P. Latha, *Annals of R.S.C.B.*, 25(2021)17361.
51. K. R. Mahanthesha, B.E. K. Swamy, U. Chandra, Y. D. Bodke, K. V. K. Pai and B.S Sherigara, *Int. J. Electrochem. Sci.*, 4 (2009) 1237.
52. U. Chandra, B. E. K. Swamy, O. Gilbert, S. S. Shankar, K.R. Mahanthesha and B.S. Sherigara, *Int. J. Electrochem. Sci.*, 5 (2010) 1.
53. K. R. Mahanthesha, B.E. K. Swamy, K.V.K. Pai, U. Chandra and B. S. Sherigara, *Int. J. Electrochem. Sci.*, 5 (2010) 1962.
54. D.K. Gosser, *Cyclic Voltammetry*, VHC, (1994) New York.
55. K.R. Mahanthesha, B.E. K. Swamy and K.V.K. Pai, *Anal.Bioanal. Electrochem.*, 6 (2014)234.
56. O. Gilbert, B.E.K. Swamy, U. Chandra and B.S. Sherigara, *J. Electroanal. Chem.*, 636 (2009) 80.
57. M. Li, F. Ni, Y. Wang, S. Xu, D. Zhang, S. Chen and L.Wang, *Electroanalysis*, 21 (2009)1521.
58. P.S. Ganesh, B.E.K. Swamy and Rekha, *Sci. Lett. J.*, 5 (2016) 236.
59. D.M. Zhao, X.H. Zhang, L.J. Feng, L. Jia and S.F.Wang, *Colloids Surf. B*, 74 (2009) 317.
60. W. Si, W. Lei, Y. Zhang, M. Xia, F. Wang and Q. Hao, *Electrochim. Acta*, 85 (2012) 295.
61. Y. Zhang, R. Sun, B. Luo and L. Wang, *Electrochim. Acta*, 156 (2015) 228.
62. K. R. Mahanthesha and B. E. K. Swamy, *Anal. Bioanal. Electrochem.*, 10 (2018)321.
63. M. Kumar, B.E. K. Swamy, B.Hu, M. Wang, G. Yasin, B. Liang, H.D. Madhuchandra and W. Zhao, *Microchem.J.*, 168(2021)106503.